

Determination of Metal Nanoparticle Size Distribution in Gold Hydrosols of Plasmonic Absorption Spectra

I.M. Bolesta^{1,*}, R.V. Gamernyk¹, O.M. Shevchuk², O.O. Kushnir¹, I.I. Kolych¹,
T.E. Konstantinova³, A.S. Zaichenko²

¹ Ivan Franko National University of Lviv, 1, Universytetska Str., 79017 Lviv, Ukraine

² Lviv Polytechnic National University, 12, S. Bandera Str., 79013 Lviv, Ukraine

³ Donetsk Institute for Physics and Engineering named after O.O. Galkin, National Academy of Sciences of Ukraine,
72, R. Luxembourg Str., 83114 Donetsk, Ukraine

(Received 20 November 2012; published online 29 December 2012)

The method for determination of the metal particle size distribution based on the optical absorption data for composites consisting of dielectric medium and metallic inclusions is substantiated. The mentioned method is tested on hydrosols of gold nanoparticles by comparison with the data obtained by the microscopic investigations.

Keywords: Hydrosols of gold, Metal clusters, Plasmon resonance, TEM, Absorption spectra.

PACS numbers: 73.20.Mf, 81.07.Bc

1. INTRODUCTION

Nanoparticles of noble metals, such as gold and silver, possess unique physical and optical properties, which are defined by their size and shape, distance between particles, nature of protective organic cover [1]. Therefore, such nanoparticles and their colloidal solutions find application in different fields: radio- and photoelectronics (metal-containing coatings, composites, and functional pastes), for the creation of devices of nonlinear optics, in catalysis of chemical and biological processes, in biochemistry and cell biology as biomarkers, analytical reagents for separation and extraction of cell cultures, for targeted drug delivery, genetic material delivery to cell nucleus by the method of biolistic transfection, visualization of cell structures, diagnostics and medical treatment of cancerous diseases [2-4].

Fast progress of applications of nanoparticles makes very promising the problem of development of methods which would allow to estimate the size and, especially, size distribution of synthesized nanoparticles. The atomic-force and transmission electron microscopies are usually used for this purpose [5]. However, these methods, which are inherently the local ones, require a special procedure of sample preparation, and, so, they cannot be directly applied for the determination of particle distribution in soles that is a promising problem of biotechnology [6]. Dynamical light scattering (DLS) method [7] is one of the possible methods which are used during last years for the determination of particle sizes in solutions and soles. However, it is necessary to have the corresponding complex equipment for its realization and this method also has certain limitations [8].

Therefore, the aim of the present work is the development and substantiation of the express-method for the determination of sizes and distribution of nanoparticles by means of the mathematical processing of the absorption spectra of their hydrosols in the UV- and visible spectral regions.

2. METHODS OF SYNTHESIS AND EXPERIMENT

For the realization of the assigned task, we have used the synthesis method of gold nanoparticles by chemical reduction from solutions of HAuCl_4 soles in micelle-like structures formed by oligomeric surface-active compounds which act as "exotemplates" limiting nanocrystal growth [9, 10]. This gives the possibility to synthesize nanoparticles with controllable size and size distribution. Linear heterofunctional oligoperoxide (HFO) based on N-vinylpyrrolidone (N-VP), peroxide monomer of 5-tret-butylperoxi-1-methyl-1-hexene-3 and dimethylaminoethyl methacrylate (DMAEM) was used as the surface-active substance being exotemplate in synthesis of gold nanoparticles. Two types of hydrosols (type 1 and type 2) of gold nanoparticles with different metal particle size distributions were obtained by the mentioned technique.

Electron-microscopic investigations were carried out on the transmission electron microscope JEM-200A of "JEOL" at the accelerating voltage of 200 kV. Samples for the electron-microscopic studies were produced by spraying on the substrate (thin carbon film deposited on copper grid) by using the US disperser "Ultrasonic Disintegrator" UD-20 for deagglomeration of particles.

Computer programs which automatically determine the particle size on image were developed for the image processing. To define the particle position we have used the water-parting method [11] for the brightness representation of the TEM image. Separation of the particle boundaries was performed by the method of auto select of a brightness threshold [12] for each region separated by the water-parting method. Equivalent radius r_{eq} for particles was determined as the circle radius whose area coincides with the particle area S , i.e. $r_{eq} = \sqrt{S/\pi}$. In order to calculate the particle area S , one should only determine the number N_p of image points involving to the region which corresponds to a particle and multiply the discretization interval along the x - and y -axes as the following: $S = N_p \Delta x \Delta y$.

* bolesta@electronics.wupl.lviv.ua

Position of the particle center was determined as a point, from which the root-mean-square distance for the image points representing the given particle is minimum. Coordinates of this point, obviously, can be inconsistent with a grid of the AFM image. Information about coordinates of the particle centers allows to obtain such an important parameter as the distance between the nearest neighbor particles r_{dbn} . It is determined by a direct enumeration of the distance from the chosen particle to each other on the image.

Absorption spectra of hydrosols of Au nanoparticles were measured on the spectrophotometer Specord-M40 in the parallel-plate cell ($d = 10$ mm). The reference cell was filled by water solution of HFO.

3. MODELING OF THE SPECTRA AND DISTRIBUTION CALCULATIONS

Spherical shape of gold nanoparticles in dielectric medium allows to calculate the extinction cross-section in the theory of Mi [13], according to which the effective extinction cross-section $C_{ext}(\lambda, r)$ for a sphere of the radius r is determined by the correlation [14]:

$$C_{ext}(\lambda, r) = \frac{2\pi}{k^2} \sum_{n=1}^{\infty} (2n+1) \operatorname{Re}(a_n + b_n), \quad (3.1)$$

where $k = 2\pi/\lambda$. Coefficients a_n and b_n are given by the following equations:

$$a_n = \frac{m^2 j_n(x) [x j_n'(x)]' - j_n(x) [m x j_n'(mx)]'}{m^2 j_n'(mx) [x h_n^{(1)}(x)]' - h_n^{(1)}(x) [m x j_n'(mx)]'}, \quad (3.2)$$

$$b_n = \frac{j_n(x) [x j_n'(x)]' - j_n(x) [m x j_n'(mx)]'}{j_n'(mx) [x h_n^{(1)}(x)]' - h_n^{(1)}(x) [m x j_n'(mx)]'}, \quad (3.3)$$

where stroke denotes derivative of the argument; $j_n(x)$ and $h_n^{(1)}(x)$ are the spherical Bessel and Hankel functions; $x = kr$ is the product of the wave vector modulus and nanoparticle radius; $m^2 = \varepsilon/\varepsilon_m$ is the relative complex permittivity of the particle material (here ε_m is the permittivity of the environment).

In the case of nanodimensional metal particles, their permittivity becomes dependent on the sizes. This is connected with the decrease in the electron mean free path due to its collisions with the particle surface [15, 16]. In this case, dimensional dependence of the relative permittivity is described by the expression [16]

$$\varepsilon(r) = \varepsilon_{\infty} + \frac{v_F A_{size}}{r}, \quad (3.4)$$

where ε_{∞} is the permittivity of a bulk material; v_F is the electron Fermi velocity (for gold $v_F = 1,40 \cdot 10^6$ m/s); A_{size} is the phenomenological dimensional parameter. The data of ε_{∞} from [17] was used in the calculations. The value of dimensional parameter A_{size} is in the range from 0,25 (for vacuum) to 3,6 [18]. We have obtained $A_{size} = 1,75$ for the first hydrosol (type 1) and 1,25 for the second hydrosol (type 2).

The essence of the method for the calculation of the particle radius distribution consists in the minimization of the root-mean-square deviation between the experimental and calculated extinction spectrum of the studied system of nanoparticles.

A predictable set of n particle radiuses, for example, from 1 nm to 20 nm with the step of 1 nm, which are depicted by the column vector $R = (r_1, r_2, \dots, r_n)^T$ (T is the operation of transportation), was chosen for its realization. Extinction spectra in the wavelength range, where experimental spectra were measured, were calculated for all particles with the chosen radiuses based on the Mi theory.

Experimental spectrum is also represented by the column vector E in the "space" of wavelengths which contains m components for λ_i ($i = 1, \dots, m$). Calculated spectra C_{ji} ($j = 1, \dots, n$; $i = 1, \dots, m$) in this "space" form matrix with n columns and m rows, each element C_{kl} of which specifies the extinction value of the sphere of the radius r_k on the wavelength λ_l .

At such representation each point of the experimental dependence E_l on the wavelength λ_l can be approximated by a linear combination of the calculated extinction values C_{jl} ($j = 1, \dots, n$) on the chosen wavelength λ_l :

$$E_l = \sum_{j=1}^n C_{jl} \omega_j, \quad (3.5)$$

where ω_j is the weight of the contribution of the j -th particle to the total spectrum that is formed by column vector W . Then approximation of the experimental spectrum E is achieved by the minimization method of the root-mean-square deviation

$$S = \sum_{i=1}^m \left(E_i - \sum_{j=1}^n C_{ji} \omega_j \right)^2, \quad (3.6)$$

which, according to [19], is reduced to matrix equation

$$C^T(CW - E) = 0. \quad (3.7)$$

The last equation can be re-written in the form of

$$FW = T, \quad (3.8)$$

where designations $F = C^T C$, $T = C^T E$ are introduced.

Approximation accuracy was defined from the root-mean-square deviation by the following formula:

$$\delta = \frac{\sqrt{S}}{\sum_{i=1}^m |E_i|}. \quad (3.9)$$

4. EXPERIMENTAL RESULTS AND DISCUSSION

In Fig. 1 we show the TEM photographs of two types of gold hydrosol, on which conducting metal particles are clearly distinguished. Processing of the images using the created programs allowed to obtain numerical parameters of the investigated objects.

In Fig. 2 we illustrate the particle radius distribution of both hydrosols. As seen, maximum of the nanoparticle size distribution in the hydrosol of type 1 is found to be in the region of 4-5 nm, and in the hydrosol of type 2 – 2-3 nm. Approximation of the distribution curves is well realized by the Gauss curve, whose half-width value gives 4 nm (type 1) and 2 nm (type 2). It is follows from the aforesaid that hydrosol of type 2 is more monodisperse in comparison with type 1.

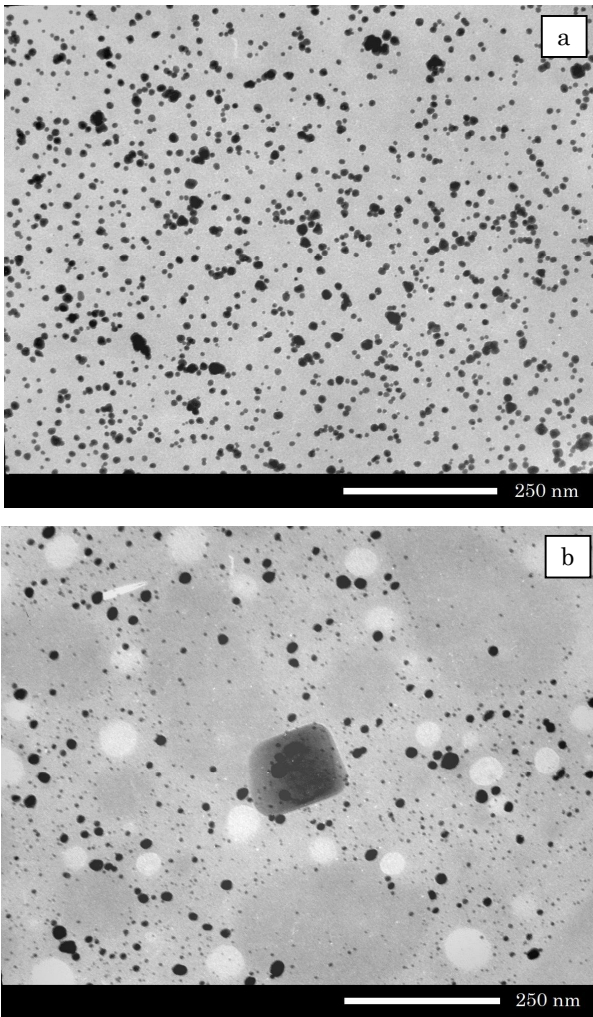


Fig. 1 – Electron-microscopic images of the gold hydrosols of type 1 (a) and type 2 (b)

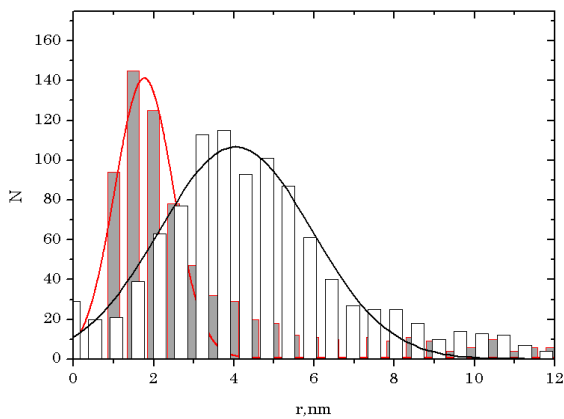


Fig. 2 – Particle radius distributions for hydrosols of type 1 (light columns) and type 2 (dark columns). Solid curves are the approximation of the experimental size distributions by Gauss function

In Fig. 3 we represent distributions by the distances between nanoparticles for the same hydrosols. As seen, distributions are approximately the same with maximum in the region of 10-15 nm. As it follows, the distances between nanoparticles considerably exceed their sizes, and this allows to not take into account the interaction between nanoparticles. Condition of non-interaction is

one of the main in the Mi theory [14], and, therefore, its application in calculations of the spectra of the studied hydrosols is reasonable.

In Fig. 4 we show the experimental extinction spectrum of gold hydrosols, on which absorption bands with maximums of 524,9 nm (type 1) and 526,0 nm (type 2) are clearly fixed. These bands are connected with the surface plasmon resonance in gold nanoparticles. Really, position of the resonance frequency of surface plasmon band for a spherical metal nanoparticle in dielectric medium is determined from the Frohlich condition [20]

$$\text{Re}[\varepsilon(\omega)] = -2\varepsilon_m, \quad (4.1)$$

where $\varepsilon(\omega)$ is the permittivity of metal (in the given case, of gold); ε_m is the permittivity of environment. Using the frequency dependence of the refraction coefficient of water solution of HFO n_m [21] and substituting data for the optical properties of gold [17], we obtain the resonance frequency in the vicinity of 522-524 nm. The found value of the resonance frequency coincides well with the maximums of the experimental spectra that confirms the suggestion about connection between absorption bands and surface plasmon resonance in gold nanoparticles.

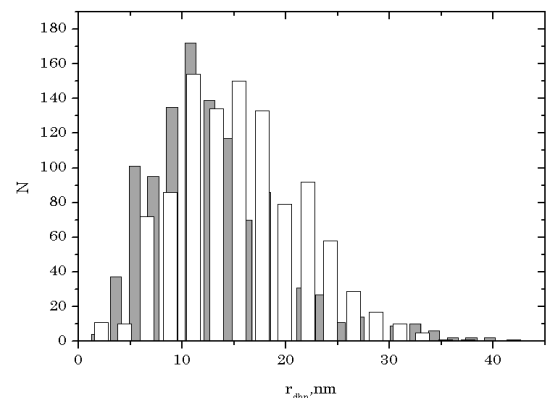


Fig. 3 – Distributions by the distances between particles for hydrosols of type 1 (light columns) and type 2 (dark columns)

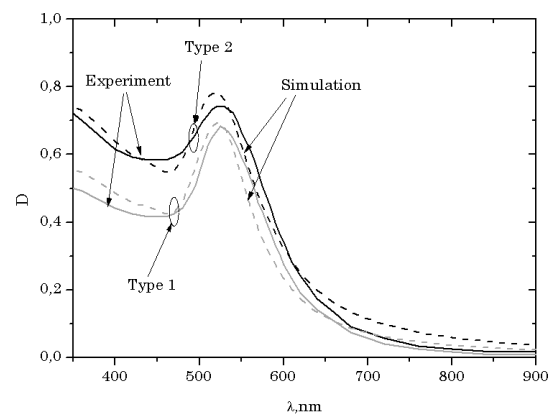


Fig. 4 – Experimental (solid curves) and modeled (dashed curves) extinction spectra of gold hydrosols of type 1 (black curves) and type 2 (grey curves)

Spectra of the corresponding hydrosols calculated from the Mi theory are depicted in Fig. 4 by the dotted lines. It is seen that the calculated spectra coincide with the accuracy of 6,0% (type 1) and 5,2% (type 2). Long-wave decay of the calculated spectra is shifted to the

region of smaller wavelengths that can indicate an insignificant interaction between particles which are not far away (see Fig. 3).

In Fig. 5 we illustrate the calculated particle size distributions obtained by using the above described technique. Gauss approximation of the experimental distributions (solid lines in Fig. 2) is given in this figure for the comparison.

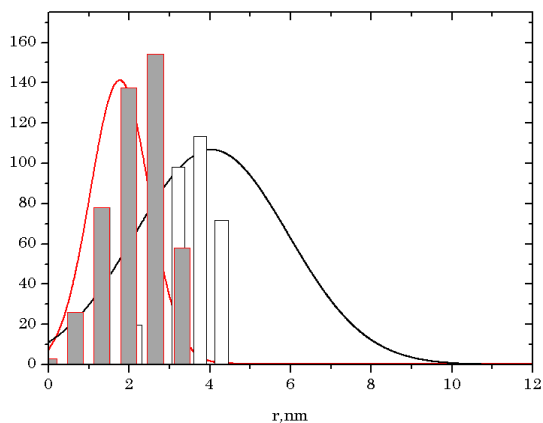


Fig. 5 – Size distributions of gold particles in hydrosols obtained by the approximation of the optical spectrum for type 1 (light columns) and type 2 (dark columns) of hydrosols. Solid curves are the approximation of the experimental size distributions by the Gauss function

REFERENCES

1. M. Brust, C.J. Kiely, *Colloid. Surface A* **202**, 175 (2002).
2. M.-C. Daniel, D. Astruc, *Chem. Rev.* **104**, 293 (2004).
3. L.A. Dykman, V.A. Bogatyrev, *Usp. Khim.* **76**, 199 (2007).
4. I.H. El-Sayed, X. Huang, M.A. El-Sayed, *Nano Lett.* **5**, 829 (2005).
5. A.M. Schrand, S.A.C. Hens, O.A. Shenderova, *Crit. Rev. Solid State* **34**, 18 (2009).
6. B.J. Berne, R. Pecora, *Dynamic Light Scattering* (New York: Wiley: 1976).
7. A.E. Aleksenskiy, A.V. Shvidchenko, E.D. Eidelman, *Pis'ma v ZhTF* **38**, 1 (2012).
8. A. Zaichenko, N. Mitina, O. Shevchuk, O. Shapoval, R. Bilyy, R. Stoika, A. Voloshinovskii, D. Horak, *AIP Conf. Proc.* **1275**, 178 (2010).
9. O.S. Zaichenko, O.M. Shevchuk, N.E. Mitina, Pat. 98430, C08K 3/08, C01G 7/00, Opubl. 10.05.2012, Bul. No9.
10. A. Zaichenko, S. Voronov, O. Shevchuk, V. Vasilyev, A. Kuzayev, *J. App. Polym. Sci.* **67**, 1061 (1998).
11. S.H.K. Malik, A. Khan, A. Bibi, *J. Inf. Sci. Inf. Technol.* **6**, 546 (2009).
12. R.E. Woods, R.C. Gonzalez, *Digital Image Processing* (New Jersey: Prentice Hall: 2008).
13. C.F. Bohren, D.R. Huffman, *Absorption and scattering of light by small particles* (New York: Wiley: 1998).
14. G. Mie, *Ann. Physik* **25**, 377 (1908).
15. A.V. Pinchuk, U. Kreibig, A. Hilger, *Surf. Sci.* **557**, 269 (2004).
16. A. Hilger, M. Tenfelde, U. Kreibig, *Appl. Phys. B* **73**, 361 (2001).
17. P.B. Johnson, R.W. Christy, *Phys. Rev. B* **6**, 4370 (1972).
18. U. Kreibig, M. Gartz, A. Hilger, R. Neuendorf, *Nanostruct. Mater.* **11**, 1335 (1999).
19. L.I. Turchak, P.V. Plotnikov, *Osnovy chislennyh metodov* (M.: Fizmatlit: 2002).
20. S.A. Maier, *Plasmonics: Fundamentals and Applications* (New York: Springer: 2007).
21. G.M. Hale, M.R. Querry, *Appl. Opt.* **12**, 555 (1973).